21, rue d'Artois, F-75008 PARIS
http : //www.cigre.org

CIGRE US National Committee
2015 Grid of the Future Symposium

Novel Simulation Method to Quantify Induced Voltage & Current between Parallel or Partially Parallel Proximity AC Transmission Circuits

X. WU, D. MEISNER, V. SIMHA, R. WELLMAN
American Electric Power
USA

SUMMARY

Utility lineman working on de-energized lines may still be exposed to potentially hazardous induced voltages if they are in close proximity to energized, high voltage lines. Additionally, placing and removing temporary safety grounds (TPGs) may further expose workers to pre-arcing and arcing due to induced voltage and currents. Double-circuit transmission lines on shared structures are of special concern due to reduced separation distance between the conductors of adjacent lines. In order to develop safe working procedures for line maintenance it would be useful to calculate the induced voltages and currents on de-energized lines due to electrostatic and magnetostatic line coupling. This paper focuses on theoretical analysis and simulation methods of parallel and partially parallel transmission circuits to calculate induced voltage and current in de-energized AC transmission lines. An innovative approach is presented using CDEGS (Current Distribution, Electromagnetic Fields, Grounding and Soil Structure Analysis) software to study a complex line case. The results are shown and discussed including a comparison with a field measurement. In addition, a method is detailed to calculate the coupling effect of both the parallel and unparallel sections of adjacent transmission lines using the CDEGS software. This approach addresses a need in the utility industry to help quantify the effects of electrostatic and electromagnetic coupling in complex line configurations.

KEYWORDS

Induced Voltage, Induced Current, Line Coupling, Partially Parallel

xwu@aep.com

INTRODUCTION

Electrostatic and magnetostatic coupling can cause serious safety concerns for personnel maintaining a de-energized power line located in the vicinity of an energized line. Temporary protective grounds (TPGs) are typically used for de-energized transmission line work according to OSHA rules [1]. Installing or removing TPGs is a slow switching (manual) movement, which may produce an electric arc. Furthermore, linemen should follow a specific sequence when installing and removing TPGs. Due to the effects of air ionization and plasma behaviour, the removal of the TPGs (arc interruption) presents greater challenges than TPG installation (pre-arcing). Two arc interrupting scenarios are considered in this paper: Scenario 1) removal of the second to last TPG when only one TPG is still connected to the de-energized line; and Scenario 2) removal of the final TPG from the de-energized line.

Manually removing a TPG with a hot stick may lead to a long electrical arc. Although environmental factors such as wind, temperature and humidity play a role; the electrical parameters of recovery voltage and interrupting current are most significant to predict arc behaviour. Additionally, these electrical parameters are dependent on the physical line arrangement and electrical system, and then can be calculated, while the environmental factors cannot be predicted or controlled as easily. Therefore, it is important to calculate the induced voltage and current to decide if further mitigations are needed to extinguish the arc. For example, permanent ground switches could be installed at the remote substation line ends or a mobile ground switch/breaker could be utilized for removal of the final temporary grounds, removing workers from the arc zone.

There are some previous researches on this topic. Horton published a transaction paper in 2008 with a detailed introduction of induced voltage and current causes and concerns [2][3]. Horton presented a method using WinIGS to simulate line coupling and compared the results with field measurements. Mousa used some calculations and analysis to propose a new grounding procedure for TPGs, which has influenced current OSHA rules for more than thirty years [4]. In addition, the induced voltage and current concepts in this paper are consistent with references [6][7].

ELECTROSTATIC AND MAGNETOSTATIC LINE COUPLING THEORY

Whenever a de-energized line is parallel to one or more energized transmission lines, voltages and currents will be induced in the de-energized line. Induced voltages and currents can be caused by both electric field and magnetic field interactions. Electrical field effects are referred to as electrostatic (or capacitive) coupling and magnetic field effects are referred to as magnetostatic (or inductive) coupling.

In Fig. 1 three simplified theoretical configurations are shown. Each configuration shows an energized line (line *a*) that is parallel to a de-energized line (line *b*). In Fig. 1a the de-energized line is floating with no TPG connected, in Fig. 1b a single TPG is connected at one end of the working zone for the de-energized line, and in Fig. 1c a TPG is connected to each end of the working zone for the de-energized line. In each configuration line *b* is assumed to be continuously parallel for its entire length to line *a*.

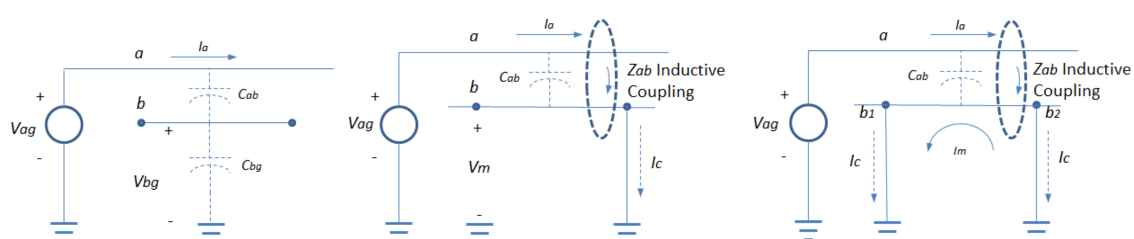

(a) (b) (c)

Figure 1. Coupling effects between an energized and de-energized line with no TPGs installed (a), one TPG installed (b), and two TPGs installed (c).

In Fig. 1a the line is mainly affected by electrostatic effects due to capacitive coupling, thus line *b* is considered to be floating at a constant, induced voltage (V_{bg}). Magnetostatic coupling is negligible as line *b* is only referenced to ground through capacitance making the series inductance of the de-energized line very high. For this configuration the length of line *b* (L_P) does not affect the open-circuit voltage as shown in Equation (1). The open circuit voltage is determined by line *a* voltage (V_{ag}), the capacitance between lines (C_{ab}), and line *b* capacitance to ground (C_{bg}).

$$V_{bg} = \left(\frac{C_{ab} \cdot L_P}{C_{ab} \cdot L_P + C_{bg} \cdot L_P} \right) V_{ag} = \left(\frac{C_{ab}}{C_{ab} + C_{bg}} \right) V_{ag} \tag{1}$$

Where:

V_{bg} = electrostatically induced, rms voltage of de-energized line *b* due to capacitive coupling;
C_{ab} = unit capacitance between line *a* and line *b* in farads per meter;
C_{bg} = unit capacitance from line *b* to ground in farads per meter;
L_P = continuously parallel length of de-energized line in meters;
V_{ag} = line to ground rms voltage of the energized line *a*.

In Fig. 1b a temporary protective ground is connected to one end of line *b*. Both electrostatic and magnetostatic coupling are present in this configuration. Electrostatic coupling results in a capacitive charging current (I_c) based on the line to line capacitance (C_{ab}) and line *a* voltage (V_{ag}) as shown in Equation (2). Magnetostatic coupling induces a distributed voltage along line *b*. The line will be at ground potential at the point where the TPG is installed and the induced voltage (V_m) at a specific distance (L_{wz}) away from the TPG is based on the mutual impedance between lines (Z_{ab}) and line *a* current (I_a) as shown in Equation (3). Unlike the previous configuration the induced voltage and current are dependent on the length that line *b* is continuously parallel to line *a* (L_P or L_{wz}).

$$I_c = 2\pi f \cdot C_{ab} \cdot L_P \cdot V_{ag} \tag{2}$$

$$V_m = Z_{ab} \cdot L_{wz} \cdot I_a \tag{3}$$

Where:

I_c = electrostatically induced charging current; split between connected TPGs;
Z_{ab} = unit mutual impedance between line *a* and line *b* in ohms per meter;
V_m = magnetostatically induced voltage at distance L_{wz} from installed TPG;
L_{wz} = length of working zone on line *b* in meters;
For one TPG installed this is the distance from the TPG along line b;
For two TPGs installed this is the distance between TPGs.
I_a = rms current of the energized line *a*.

In Fig. 1c a TPG is connected at each end of the working zone on line *b*, forming a ground loop. Again both electrostatic and magnetostatic effects are present in this configuration. Electrostatic coupling results in a similar charging current (I_c) as shown in Equation (2), except that in this configuration the current will be divided between the two TPGs. A magnetically coupled loop current will be induced in line *b* based on the energized line current (I_a), mutual line impedance (Z_{ab}), and the self-impedance of line *b* according to Equation (4). The resulting current in the TPG is the vector sum of the electrostatically and magnetostatically induced currents and is dependent on the length of the de-energized line that is parallel to line *a*.

$$I_m = -\frac{Z_{ab}}{Z_{bb}} \cdot L_{wz} \cdot I_a \tag{4}$$

Where:

I_m = magnetostatically induced, rms loop current of line *b* between TPGs;
Z_{bb} = unit self (series) impedance of line *b* in ohms per meter.

In the Introduction, two scenarios were discussed describing arc extinction when removing temporary protective grounds. Furthermore, recovery voltage and interrupting current were described as the main parameters used to predict arc behaviour. Considering Figure 1 again, Scenario 1 can be considered as removing one of the grounds from Fig. 1c and resulting in Fig. 1b. Therefore, in Scenario 1 the recovery voltage is V_m (Fig. 1b) and the interrupting current is the vector sum of I_m and I_c (Fig. 1c).

Scenario 2 can be considered as removing the TPG from Fig. 1b and resulting in Fig. 1a. Thus, in Scenario 2 the recovery voltage is V_{bg} (Fig. 1a) and the interrupting current is I_c (Fig. 1b). For the continuation of this paper, simulations are presented that provide induced voltages and induced currents for different line configurations that are not specifically referred to as recovery voltage and interruption current. Thus, it is important to note that the recovery voltage is the resultant voltage after TPG removal and interrupting current is the TPG current prior to removal if this work is used to develop safe line maintenance procedures.

COUPLING IN PARTIALLY PARALLEL LINES

The descriptions above depict a simplified case where the entire length of the de-energized line is completely parallel to the energized line. In Fig. 1a and Equation (1) the open-circuit induced voltage on the de-energized line is not affected by the length of the line. The energized-line voltage and the separation distance between phases and shield conductors are the main factors that determine the induced voltage.

However, this scenario is basic and simple, but it does not always exist in practice. It is necessary to consider some more complex configurations such as the Fig. 2 below.

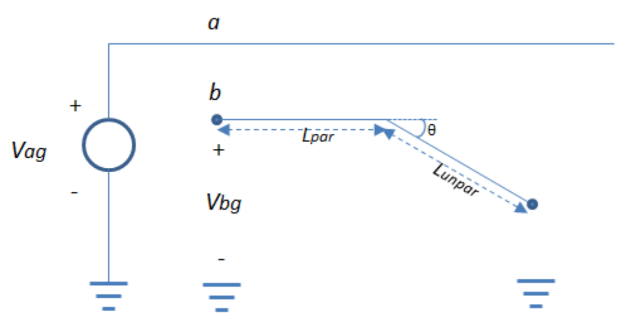

Figure 2. Simplified coupling diagram for a partially parallel line configuration.

In Fig. 2 the de-energized line *b* is not completely parallel with energized line *a* for its entire length. One section of line *b* is completely parallel with line *a*, another section of line *b* diverges from line *a* at an angle of θ. In this arrangement, the line to line capacitance (C_{ab}) and the mutual impedance (Z_{ab}) cannot be considered to be constant over the entire line length. Instead they must be represented as a function of the separation angle (θ) for the unparallel portion of line b. However, the de-energized line to ground capacitance (C_{bg}) is still constant for the entire line length. From this perspective, the unparallel section becomes less coupled to line *a* and more coupled to ground as the unparallel section increases in length.

A more complex equivalent circuit is necessary to demonstrate this line configuration. Thus, the same line configurations as presented in Fig. 1a, 1b, and 1c, are presented with an additional unparallel, de-energized line section in Fig. 3, Fig.4, and Fig. 5 respectively.

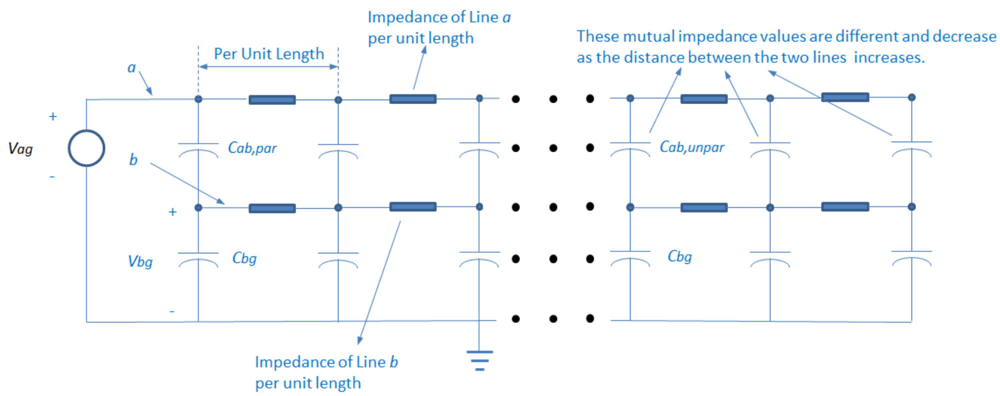

Figure 3. Distributed equivalent coupling circuit for partially paralleled lines with no TPGs installed.

In Fig. 3, there is no TPG installed on de-energized line *b*. Hence, the induced voltage on line *b* is dominated by electrostatic, capacitive coupling and magnetic field effects are negligible. The combined parallel and unparallel line capacitance can be substituted in Equation (1) to calculate induced open-circuit voltage as shown in Equation (5).

$$V_{bg} = \left(\frac{C_{ab,par} \cdot L_{par} + \int_0^{L_{unpar}} C_{ab,unpar}(l)dl}{\left[C_{ab,par} \cdot L_{par} + \int_0^{L_{unpar}} C_{ab,unpar}(l)dl\right] + \left[C_{bg} \cdot \left(L_{par} + L_{unpar}\right)\right]} \right) V_{ag} \tag{5}$$

Where,

V_{bg} = induced voltage of the de-energized line *b* due to capacitive coupling;
$C_{ab,par}$ = parallel line section unit capacitance between line *a* and line *b* in farads per meter;
$C_{ab,unpar}$ = unparallel line section unit capacitance between line *a* and line *b* in farads per meter; The unparallel line section capacitance is a function l and θ;
l = distance along unparallel section of line *b* measured from the point of divergence in meters;
θ = angle of separation between line *a* and line *b*;
L_{par}, L_{unpar} = length of parallel and unparallel line sections respectively in meters.

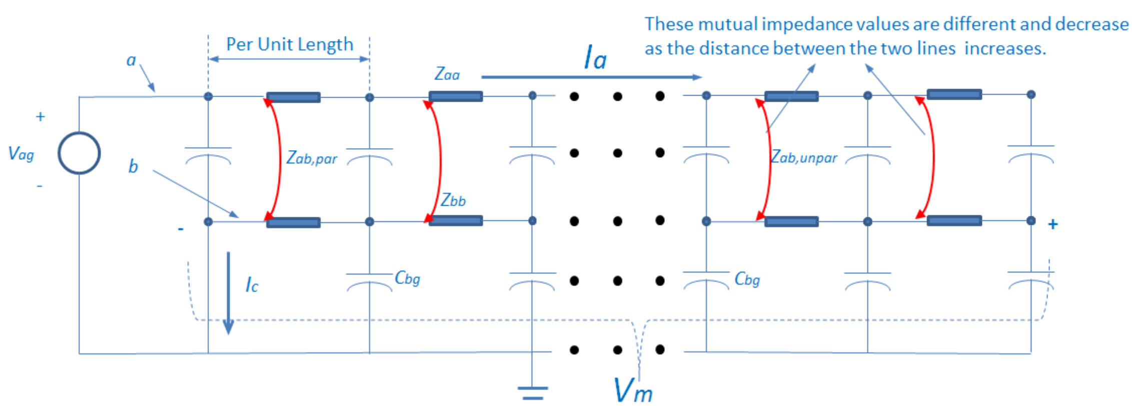

Figure 4. Distributed equivalent coupling circuit for partially paralleled lines with one TPG installed.

A single connected TPG configuration is shown in Fig. 4. In this diagram the temporary protective ground is placed at the remote end of the parallel line section. Electric field coupling will create a charging current through the TPG while magnetostatic coupling will induce a non-linear distributed voltage across the line. Substituting the total line capacitance into Equation (2) to calculate the induced charging current will yield Equation (6). Likewise, the combined mutual inductance for the parallel and unparallel sections can be substituted into Equation (3) to calculate the remote open-end voltage using Equation (7).

$$I_c = 2\pi f \cdot \left[C_{ab,par} \cdot L_{par} + \int_0^{L_{unpar}} C_{ab,unpar}(l)dl\right] \cdot V_{ag} \tag{6}$$

$$V_m = I_a\left[Z_{ab,par} \cdot L_{par} + \int_0^{L_{unpar}} Z_{ab,unpar}(l)dl\right] \tag{7}$$

Where,

$Z_{ab,par}$ = mutual impedance of parallel potion between line *a* and line *b* in ohms per meter;

$Z_{ab,unpar}$ = mutual impedance of unparallel portion between line *a* and line *b* in ohms per meter.

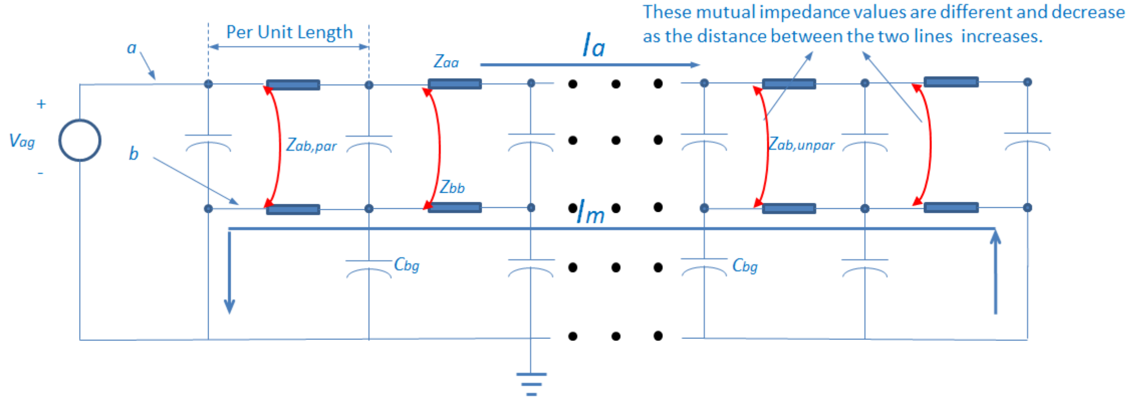

Figure 5. Distributed equivalent coupling circuit for partially paralleled lines with two TPGs installed.

When two TPGs are connected to line *b* as shown in Fig. 5, a closed ground loop is formed which creates inductive coupling resulting in loop current (I_m) to flow between TPGs. Equation (8) can be used to find the induced loop current by substituting the total line mutual impedance into Equation (4). Additionally, the total electrostatically induced charging current (I_c) will still be present in this configuration and will be equivalent to Figure 4, except the current will be unequally split between the two TPGs. The split between the TPGs will be a function of the parallel and unparallel section lengths and the angle of divergence; however, it is expected that the majority of the charging current will be flowing into the parallel section connected TPG.

$$I_m = -\left(\frac{Z_{ab,par} \cdot L_{par} + \int_0^{L_{unpar}} Z_{ab,unpar}(l)dl}{Z_{bb} \cdot \left(L_{par} + L_{unpar}\right)}\right) I_a \qquad (8)$$

SIMULATION AND COMPARISON TO FIELD RESULTS

As shown above, the ratio between the parallel section length (L_{par}) and the total de-energized line length (L_{par} + L_{unpar}) as well as the separation angle (θ) will significantly influence the effect of electrostatic and magnetostatic coupling. However, when considering a double-circuit, three phase line configuration, a capacitance and mutual impedance should be calculated for each phase conductor to all other phase conductors. Because of the difficulty in manually calculating induced voltages and currents for three phase circuits, CDEGS, a commercially available software, was used for complex line coupling simulations.

In order to prove the capability of the CDEGS software, a case from Horton was examined [2]. The same inputs were used and simulated in CDEGS and the results were compared with the field measurements provided by Horton [2].

The layout of the parallel transmission network was detailed in [2] and is shown in Fig 6. The left-structure phase conductors are energized with 115 kV, while the circuit on the right-hand side is de-energized. As a result, the de-energized phase conductors will have the induced voltages and currents due to line coupling from the energized circuit.

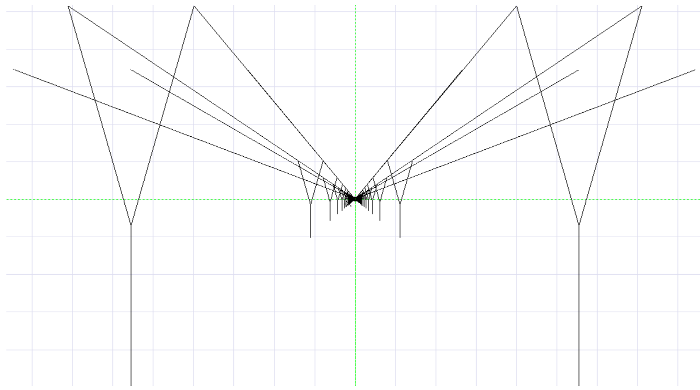

Figure 6. Corridor view of 115 kV totally parallel transmission circuits (from Horton [2])

The measured induced voltages on phase *a*, *b* and *c* of the de-energized circuit are compared to the calculated results provided by Horton in [2] using WinIGS and the simulation in CDEGS are shown in Table 1 below. In this simulation no TPGs were connected so only electric field coupling is considered.

Table 1 Comparison of Induced Voltage between Measurement and Simulation

	Phase a (kV)	Phase b (kV)	Phase c (kV)
Measured [2]	3.57	1.66	0.80
WinIGS Calculation [2]	3.80	1.79	1.02
CDEGS Calculation	3.69	1.58	0.895

Fig. 7 shows how the placement of TPGs is simulated in CDEGS. To model the TPG, the phase conductors are tied together (Jumper 1 and 2) and phase *a* is then connected directly to the closest shield wire (Jumper 3). For the CDEGS simulation, the current through Jumper 1 was calculated. However, in TPG placement and modeling in [2] some differences are noted, phase *a* was taken to the pole tower ground (not the overhead shield wire) and the induced current measurement was performed on Jumper 3 (not Jumper 1). From a practical standpoint, the conductors are tied together to form one large shorted ground loop so the differences are expected to be negligible.

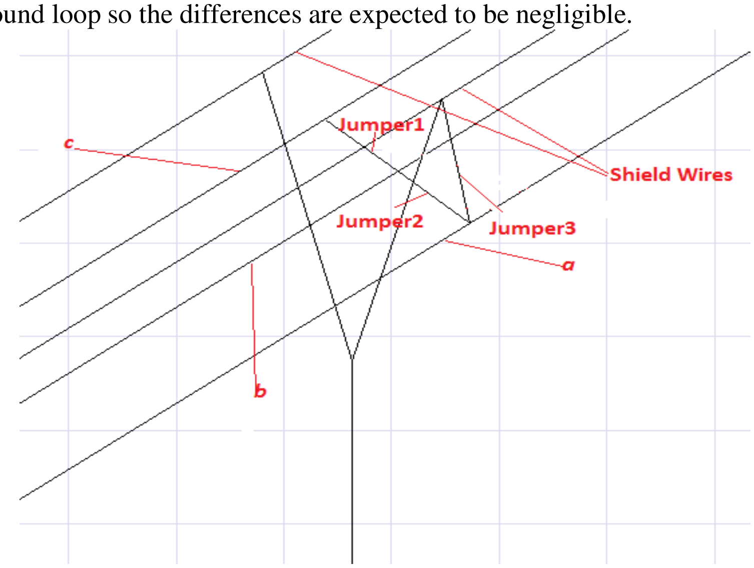

Figure 7. Ground jumpers used for CDEGS simulation of TPG.

Two induced current scenarios are shown in Fig. 8 below. In Fig. 8a one TPG is connected simulating the electrostatically induced charging current (I_1). When two TPGs are installed, the combined electrical field and magnetic field induced currents (I_2, I_3) are simulated as shown in Fig. 8b.

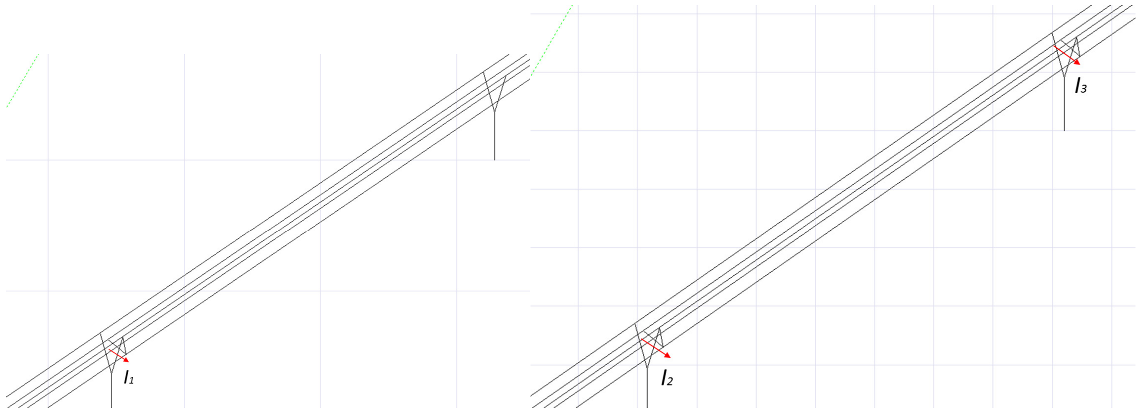

(a) (b)

Figure 8. Circuit arrangement for induced current simulation with one TPG (a) and two TPGs (b) installed on the de-energized line.

The measured induced currents and simulated results are shown in Table 2 for one and two TPGs installed on the de-energized line.

Table 2 Comparison of Induced Current between Measurement and Simulation

	I_1 (mA) One TPG	**I_2 (mA) Two TPGs (source end)**	**I_3 (mA) Two TPGs (remote end)**
Measured [2]	1090	2275	1194
WinIGS Calculation [2]	1142	2315	1248
CDEGS Calculation	1150	2290	1350

The calculated induced voltages and currents from CDEGS matched the simulations and field measurements reported by Horton well as shown in Table 1 and Table 2. The differences between the simulation and measurements are reasonable considering all assumptions and ambient measurement variables.

COMPLEX LINE CONFIGURATION CASE STUDY

An overhead plan view of a complex line configuration at AEP Station V is shown in Fig. 9. The station had multiple line exits sharing the same right of way path, including a single circuit 765 kV line, and two double-circuit 345 kV lines. The single circuit 765 kV is shown connecting to AEP Station M. An existing single circuit 345 kV line is connected to AEP Station H, with a future second 345 kV circuit planned to be added to the existing structure. Finally, a double-circuit 345 kV line on shared structures travels to AEP Station C. These lines would share the same right of way for 0.3 miles and then diverge to different stations. The five lines, including the future second circuit to Station H, were studied to determine the calculated induced voltages and induced currents that may be present during line maintenance on any of the lines.

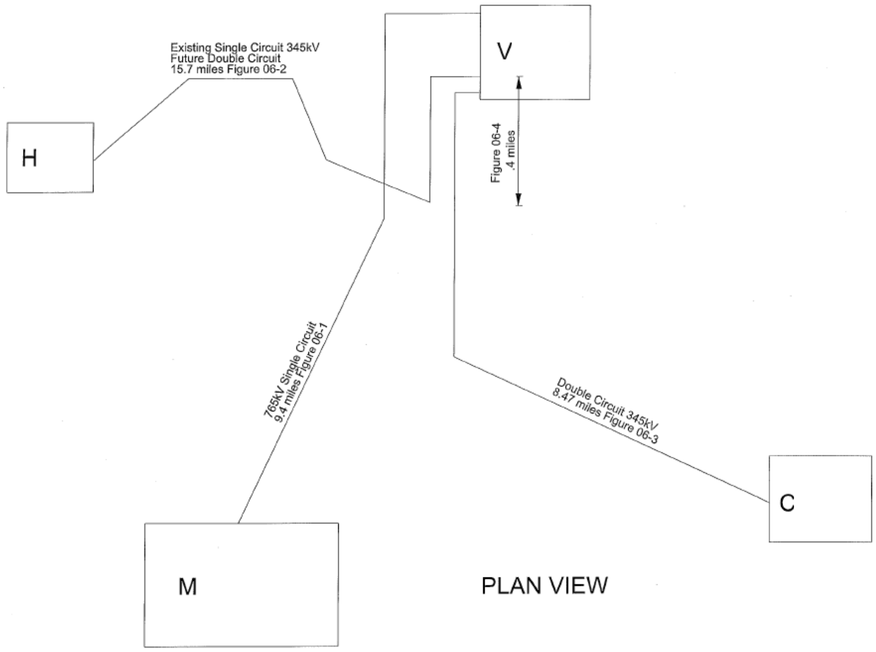

Figure 9. Plan view of adjacent lines exiting Station V showing parallel and divergent sections.

Intuitively, the coupling effects of the 765 kV circuit should be minimal. It only shares 0.3 miles in parallel with the other four circuits. Additionally, approximately 96.8% of its total 9.4-mile length is not in close proximity to any other energized circuits and the separation angle between conductors is large. The 345 kV circuits, however, have high coupling effects due to the continuous parallel paths of each 345 kV double-circuit line on shared towers.

As mentioned above, CDEGS can be used to model this complex, multiple-line configuration that includes both parallel and unparallel portions. The following assumptions are considered in this case study.

- All simulations are performed under steady-state conditions.
- All the energized circuits are under normal operation load situations.
- The lines are not transposed.
- All reactive equipment, i.e. shunt reactors, are either taken out of service or not considered.
- Ambient conditions and effects such as wind, temperature, and humidity are not considered.

The physical and electrical parameters of the transmission circuits are listed in Table 3.

Table 3 Transmission Right-of-Way Electrical & Physical Parameters

Circuit Path	V-M	V-H	V-C
Nominal Voltage	765 kV	345 kV	345 kV
Phase Normal Load Current Magnitude	200 A	267 A	245 A
Phase Conductors	1351 ACSR	954 ACSR	954 ACSR
Number/Spacing of Bundled Conductors	4/18 in	2/18 in	2/18 in
Shield Wires	7#8 Alumoweld	646 OPGW	646 OPGW
Earth Resistivity	100 Ω·m	100 Ω·m	100 Ω·m
Length	9.4 mi	15.7 mi	8.47 mi
Span Length	0.3 mi	0.3 mi	0.3 mi
Average Tower Footing Resistance	15 Ω·m	15 Ω·m	15 Ω·m

Using the configuration shown in Fig.9 and the data in Table 3, the five circuits exiting Station V were simulated in CDEGS. The simulation plan and assembly views are shown below in Fig.10.

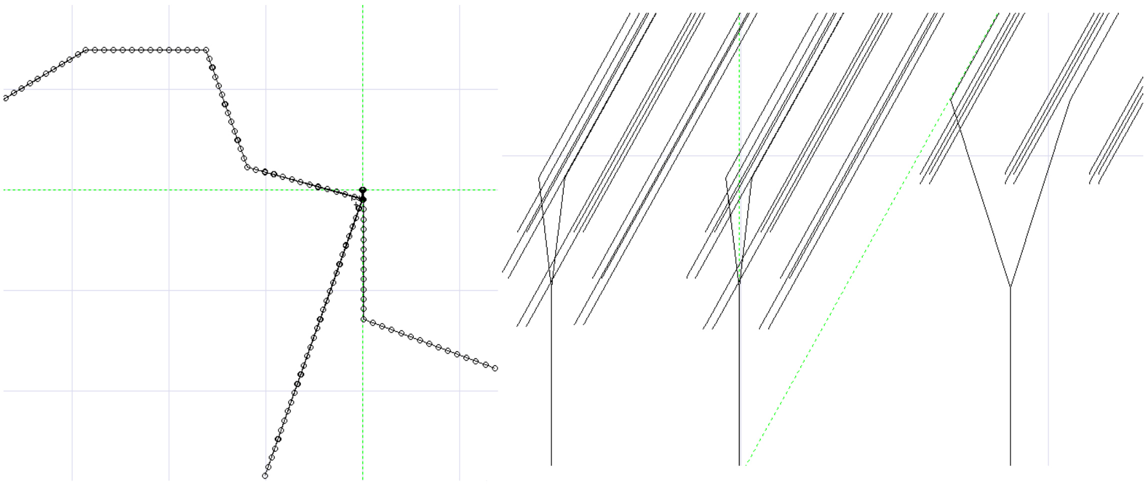

(a) (b)

Figure 10. Plan view (a) and assembly section view (b) in CDEGS for AEP Station V lines

The calculated induced voltages from the CDEGS simulation are shown below in Table 4. The induced rms voltages for phase *a*, *b,* and *c* are calculated with the circuit de-energized and all other circuits energized. In this case, electrostatic coupling is dominant and magnetic field effects are negligible, so the induced voltages represent an open-circuit case with a constant voltage across the entire line.

Table 4 Induced Voltages of Selected De-energized Circuit Phase Conductors

	Phase a (V)	Phase b (V)	Phase c (V)
M–V 765kV	50.9	86.5	179
H–V 345kV ckt1	18,663	5,093	20,882
H–V 345kV ckt2	21,306	4,845	17,922
C–V 345kV ckt1	21,070	5,146	24,175
C–V 345kV ckt2	24,257	5,624	20,684

For TPG simulation, the connection to the lines is the same as Fig. 7. The TPGs were placed on each de-energized circuit at the ends of the second span outside the shared right-of-way. Induced currents (I_1, I_2, and I_3) were calculated on each de-energized circuit with all other circuits energized. The induced currents calculated from the CDEGS model are shown below in Table 5.

Table 5 Induced Current in De-energized Circuit with TPGs Installed in Shared Right-of-Way

	I_1 (A) One TPG	I_2 (A) Two TPGs (V Station side)	I_3 (A) Two TPGs (remote end)
M–V 765kV	0.0036	0.017	0.017
H–V 345kV ckt1	1.2	20.6	21.1
H–V 345kV ckt2	1.2	21.2	21.4
C–V 345kV ckt1	0.65	20.2	20.3
C–V 345kV ckt2	0.64	20.8	21

The calculated results shown in Table 4 and Table 5 above, matched the expected results. The 765 kV single circuit line has only minor coupling effects with other lines and the parallel double-circuit line coupling effects were significant. Additional conclusions are emphasized below:

1. The induced voltage on phase *b* for the 345 kV double-circuit transmission network is always the smallest. This is because it is farthest from the energized conductors in the AEP circuit arrangement as shown in Fig. 11.

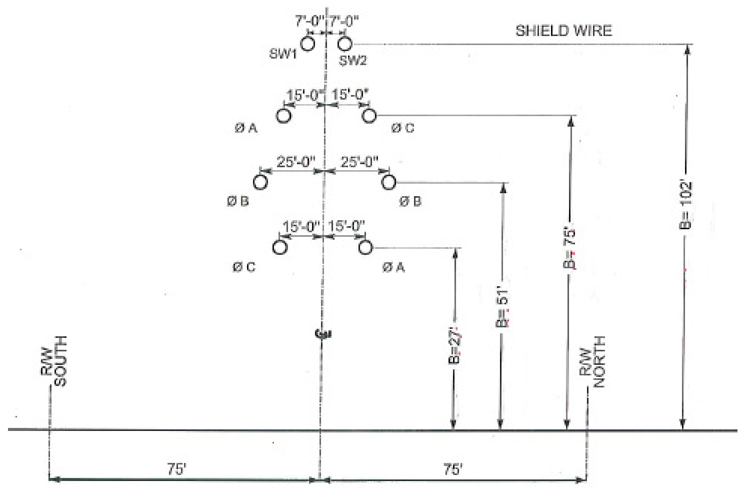

Figure 11. 345 kV double-circuit tower line arrangement

2. Furthermore, the next smallest phase voltage for 345 kV double-circuit lines will be based on the conductor's location to the shield wire. The phase that is closest to the shield wire will be more coupled to ground potential and the resulting induced voltage will be lower.
3. The electrostatically induced charging current is typically smaller than the magnetostatically induced loop current. The electrical field induced current (charging current) is very sensitive to line separation and quickly diminishes as the distance between two unparallel line sections is increased.
4. Two TPG removal scenarios are mentioned in the introduction. Based on simulation and field testing experience, the removal of the last and final TPG leads to the longest arc. Therefore, the induced voltage in Table 4 and the charging current in Table 5 are of specific interest when developing safe work practices for line maintenance work.

CONCLUSIONS & FUTURE WORK

This paper presents the theory of electrostatic and magnetostatic coupling on adjacent transmission lines. Additionally, expanded concepts including more complex line configurations with both parallel and unparallel line sections are examined. A computer simulation is presented using CDEGS software. Calculated induced voltages and currents were well matched when compared with the previous field measurements reported by Horton [2]. An AEP station case is presented to study coupling effects of a complex, five-circuit EHV line system.

The case study presented is typical for many EHV stations where line exits will share a limited right of way just outside the station prior to separating in different directions. Based on the presented case study, the coupling effect of single circuit lines in a short shared right of way will be relatively small. On the other hand, double-circuited lines with large parallel sections on shared transmission structures are subject to much higher induced voltages and currents. The induced voltages and induced currents are highly dependent on voltage, distance between adjacent line phases, distance to shield wires, and length of parallel section. As a result, it is necessary to have a method to simulate the coupling effect for parallel and partially parallel double-circuit lines.

Further work needs to be done concerning the arc behaviour when removing TPGs from a de-energized line. This work provides valuable information about the recovery voltage and interrupting current that will govern the arc extinction during manual TPG removal. However, more research is necessary to develop a better model for arc behaviour as well as develop safety criteria for removal of TPGs using a hot-stick. Further mitigation methods may be necessary if this work cannot be performed using this safety criteria. The authors intend to continue this future work for inclusion in other technical papers.

BIBLIOGRAPHY

[1] Electric Power Generation, Transmission, and Distribution, OSHA 29 CFR 1910.269.

[2] R. Horton, K. Wallace, "Induced voltage and current in parallel transmission lines: causes and concerns", IEEE Transaction on Power Delivery, Vol. 23, No. 4, Oct. 2008.

[3] R. Horton, K. Wallace, and M. Halpin, "Induced voltage in parallel transmission lines caused by electric field induction", presented at the IEEE ESMO Conf., Albuquerque, NM, 2006.

[4] A. Mousa, "New grounding procedures for work on de-energized lines eliminate the need for ground switches", IEEE Transaction on Power Apparatus and Systems, Vol. PAS-101, No. 8, Aug. 1982.

[5] "EPRI Transmission Line Reference Book 345 kV and Above", EPRI, Palo Alto, CA, 1975, Elect. Power Res. Council.

[6] H. Zhang, G.G. Karady, J. Hunt, "Effect of various parameters on the inductive induced voltage and current on pipelines", IEEE Power and Energy Society General Meeting, 2011, 1-7.

[7] Z. Wang, Q. Qiu, D. Ball, L.E. Anderson, "Case Study – Effects of Geomagnetically Induced Current (GIC) Neutral Blocking Device", presented at 2014 CIGRE Grid of the Future Symposium, Houston, TX, October 19~21, 2014